Core Loss Predictions for General PWM Waveforms from a Simplified Set of Measured Data

Charles R. Sullivan, John H. Harris
Thayer School of Engineering at Dartmouth
charles.r.sullivan@dartmouth.edu
http://engineering.dartmouth.edu/inductor
8000 Cummings Hall, Hanover, NH 03755, USA

Edward Herbert
closs@eherbert.com
http://fmtt.com/
1 Dyer Cemetery Rd., Canton, CT 06019, USA

***Abstract*—A method to generalize square-wave core-loss data to predict core loss with any common rectangular voltage waveform is proposed. An automated measurement system was used to collect the required square-wave core characterization data for ferrite and powdered-iron cores, and to collect additional data to assess the accuracy of the method for other voltage waveforms. Measurement data is presented and the application of the method in power-electronics design is discussed.**

I. Introduction

Core-loss data published by core manufacturers is based on sinusoidal excitation, whereas most applications in switching power supplies and other types of power electronics circuits use rectangular voltage waveforms. Rectangular waveforms can be described by the voltage, period, and duty cycles of the positive and negative portions of the waveform. This leads to a wide diversity of different possible test conditions, and it is not practical for manufacturers to test all possible waveforms that might be used by customers. Approximate methods to estimate expected core loss with rectangular waveforms based on sinusoidal data [1]–[8] exist, but are difficult to use, are inherently limited in accuracy, and are not in wide use in industry.

In this paper, we introduce a new approach that uses a simplified set of square-wave measurements to produce easy-to-use data that can be applied to calculate loss for any rectangular-voltage waveform. This approach is expected to provide higher accuracy than is possible starting from data based on sinusoidal waveforms, and is expected to be easier to use than existing methods for nonsinusoidal waveforms. The method can be applied to computerized optimizations or in hand calculations using graphical data. Although the data required is different from conventional sinusoidal measurements, the amount of data needed is no more than the amount of data collected in traditional loss characterization.

In order to implement and evaluate the new method, we have developed an automated excitation and data collection system under computer control. This allows rapidly gathering the proposed square-wave characterization data set, and also faciltates scanning through other rectangular waveform sets in order to assess the accuracy of the generalization from the characterization data.

Previous methods for predicting core loss with rectangular waveforms based on sinusoidal data are reviewed in Section II. The new calculation method is described in Section III and the measurement system in Section IV. Measurement results are presented and used to assess the accuracy of the method in Section V. A guide to applying the method in practical design is provided in Section VI. Section VII further discusses the future application and improvement of this approach.

II. Previous Methods for Core Loss with Nonsinusoidal Waveforms

For sinusoidal waveforms, loss is often estimated by a power law equation [9], [10]

$$\overline{P_v} = k f^{\alpha} \hat{B}^{\beta} \tag{1}$$

where $\hat{B}$ is the peak flux amplitude, $\overline{P_v}$ is the time-average power loss per unit volume, and f is the frequency of sinusoidal excitation, and k, α, and β are constants found by curve fitting. A similar equation, but without the frequency dependence, was proposed by Steinmetz in 1892 [11], and so (1) is often referred to as the Steinmetz equation. Unfortunately, the Steinmetz equation, as well as the data provided by manufacturers of magnetic materials, is based only on sinusoidal excitation, and nonsinusoidal waveforms result in different losses [1], [2], [5]. DC bias can also significantly affect loss [12], [13], [14].

More detailed models, based on physical phenomena producing loss, have been studied [15]–[18]. However, especially for ferrites, there is not yet a clear consensus on a practical physically-based model that properly includes dynamic and nonlinear effects [5].

Initial attempts to make use of Steinmetz-equation parameters and extend the calculation to address arbitrary waveforms allowed improved loss estimates, but have significant limitations. The "modified Steinmetz equation" (MSE) [1], [2], [3] works well for waveforms with small harmonic content, but exhibits anomalies with large harmonic content [5], as does the model introduced in [4],

978-1-4244-4783-1/10/$25.00 ©2010 IEEE

as discussed in [6]. The "generalized Steinmetz equation" (GSE) was introduced in [5] to overcome anomalies in the MSE, and although it overcomes the problems with the MSE, it has poor accuracy in some regions [6].

A satisfactory method of using Steinmetz-equation parameters to roughly estimate loss with non-sinusoidal waveforms, the "improved generalized Steinmetz equation" (iGSE) was introduced in [6]. The same equation was independently discovered in [7], [8], where it was called the natural Steinmetz extension (NSE). Comparisons of different approaches in [24] confirm results in [6], [7], [8] showing that this method can work well in many situations.

An additional refinement introduced in [6] is to decompose a waveform that includes minor loops in the hysteresis curve, and separately analyze the loss in each minor loop. This was shown to be essential for accurately modeling such cases. An automated algorithm is described in [6] to perform this decomposition, but is unnecessary for waveforms without minor loops.

Despite these improvements, the iGSE remains an approximate prediction method, and, in particular, is dependent on the accuracy of the underlying Steinmetz model for sinusoidal loss. Unfortunately, the best-fit Steinmetz parameters are known to vary with frequency [25], [5]. For waveforms with a harmonic content over a wide frequency range, choosing the appropriate parameters can be problematic [5]. Some solutions to this problem that work for sinusoidal waveforms (e.g., [25], [26]) are not applicable with the iGSE. Summing several power-law terms is one option that can be used to better capture the wide-range frequency behavior while retaining compatibility with the general approach of the iGSE, at the price of additional complexity [7].

The approach in this paper is to directly measure loss with square waveforms, rather than trying to extend data from sinusoidal loss measurements to square waveforms. The advantages relative to the iGSE and related methods are both simplicity and accuracy. The challenge to developing such a method is to be able to take data for a reasonably constrained set of parameters, and be able to use the results to predict loss for a wider range of practical waveforms. This is discussed in the next section.

III. Calculating Core Loss from a Simplified Data Set

Consider a core with voltage waveforms such as those shown in Fig. 1, typical of power electronics applications, applied to a winding. The flux in the core will ramp up or down during each positive or negative voltage pulse, respectively. We hypothesize that the energy loss incurred during each of these flux transitions depends only on the amplitude and duration of the pulse, and that there is no loss during periods of zero applied voltage (constant flux). If this is the case, we can decompose any of the rectangular waveform types shown in Fig. 1(b) into a set of two pulses,

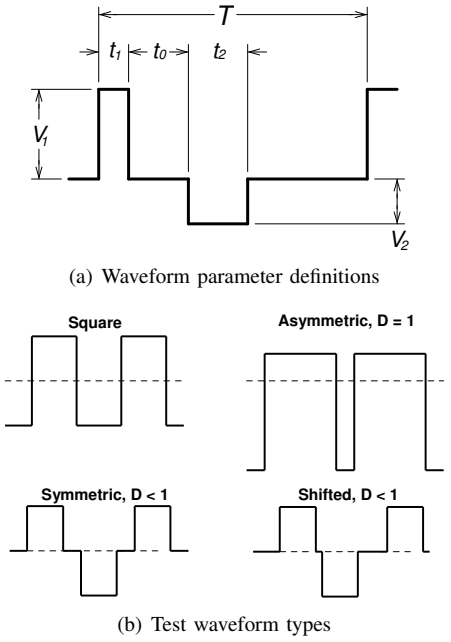

(a) Waveform parameter definitions

(b) Test waveform types

Fig. 1: Waveforms (voltage vs. time): parameters and test waveform types. Square waves are used for characterizing materials; the other test waveforms are used to test the validity of the composite waveform hypothesis.

calculate the energy loss associated with each pulse, and sum them to find the total energy loss per cycle. We call this hypothesis the *composite waveform hypothesis*.

If the composite waveform hypothesis proves to be a good approximation, we can predict core loss for any of the waveforms in Fig. 1(b) if we know the loss for a square pulse as a function of its amplitude and duration. While we might estimate that loss from sinusoidal data using one of the methods describe in Section II ([1]–[8]), a more accurate approach is to collect measured test data with square voltage waveforms, for which we can assume that the loss associated with each pulse is one half of the per-cycle energy loss. This requires data as a function of two parameters, such as flux amplitude and frequency, as used in conventional sinusoidal loss characterization. The parameters may also be described in terms of applied voltage per turn (corresponding to flux ramp rate) and on-time t_1 (one half the period for square waves).

The method we propose starts with characterizing a core material by measuring loss data for square waveforms. One half of the measured energy loss per cycle is the energy lost for a single pulse of the applied amplitude and on-time. If the composite waveform hypothesis is accurate, the same loss per cycle will be incurred for that applied voltage and on-time in any composite waveform. For the waveforms we consider here (Fig. 1), the waveform comprises two pulses. To find the total energy loss per cycle one sums the per-

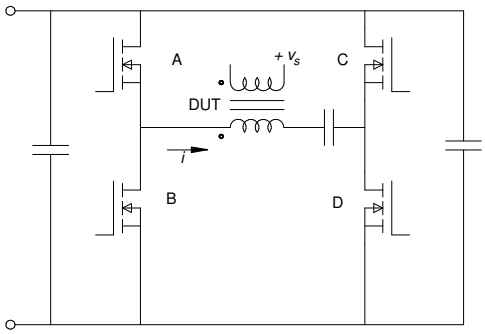

Fig. 2: Full-bridge excitation circuit. The device under test, a magnetic core, is labeled DUT.

TABLE I: Sample cores.

Manufacturer	Part	Material	Turns used
Magnetics	42206-TC	R ferrite	5
Micrometals Inc.	T80-52	–52 iron powder	21

pulse loss data for each of the two sets of pulse parameters (amplitude and on-time) from the corresponding square-wave measurements.

In Sections IV and V we report on experimental measurements conducted for two purposes: 1) to collect square-wave data for sample cores as is necessary for this method, and 2) to assess the accuracy of the method and of the composite waveform hypothesis. We note that all of the previous methods for predicting loss with non-sinusoidal waveforms discussed in Section II depend on some version of the composite waveform hypothesis, even though this assumption is rarely stated. Thus, tests of this hypothesis are important for other approaches to predicting non-sinusoidal losses as well as for validating the approach proposed here.

Predictive core loss models built up from fundamental physical principals are not available for most core loss mechanisms, and so theoretical analysis of the composite waveform hypothesis is not possible. However, for core loss produced purely by classical eddy-current effects, physical models are well established, and analytical solutions exist for some geometries. It can be shown that, for classical eddy-current loss in core material layers thicker than or comparable to an electromagnetic skin depth, the composite waveform does not always hold exactly. However, it may still be a useful approximation, and may hold exactly for other types of losses. Thus experimental evaluation is needed to assess its utility.

IV. Measurement System

We use a two-winding loss measurement [8] on toroidal core samples with 5 or 21 turns to match core characteristics to our drive system capabilities. The drive winding is connected to a full-bridge switching network through a blocking capacitor (Fig. 2). The gates of the four MOSFETs are controlled by an arbitrary function generator through a logic circuit and optically isolated gate drivers. Both the arbitrary function generator and the dc power supply feeding the bridge circuit are automatically controlled by a computer to allow synthesis of a sequence of different rectangular voltage waveforms.

Current in the drive winding is sensed with a Tektronix P 6021 wide-band passive ac current probe. This avoids the delay inherent in an active current probe; delay measurements verify that the delay is negligible. Flux is calculated from the voltage v_s across a sense winding. These signals are acquired by a digital storage oscilloscope under computer control to automatically collect waveforms from a sequence of measurements. After the waveforms are allowed to reach steady-state, 512 periods are averaged, and the average is recorded with 1000 points per period. Core loss and other parameters are calculated off line from the acquired data.

The core temperature can be controlled by immersion in a heated oil bath. All the results reported here are for an oil-bath temperature of 80 °C. The automated data collection allows acquiring data for a single excitation in less than two seconds; a pause of about two seconds precedes the next excitation. Even without the oil bath, this results in very little temperature rise; with the oil bath, temperature deviations are negligible.

For verification of the test system, a large air-core toroidal transformer was constructed. This would, in principle, provide a zero-core-loss reference. However, large stray capacitance in the transformer led to excessive ringing in the waveforms and negative power dissipation numbers. Future work will develop a better reference design to allow a useful air-core test.

V. Experimental Results

Two sample cores were tested: one ferrite core and one powdered-iron core, as listed in Table I.

A. Characterization

Fig. 3 presents square-wave loss data in two different formats for the ferrite core. Fig. 3(a) uses a format similar to that used for sinusoidal loss data on many datasheets. Fig. 3(b) shows a Herbert curve in which core loss is plotted as a function of on-time (t_1 in Fig. 1(a)), parameterized by the voltage per turn during that on-time [27]. The Herbert curve is convenient for use in design as discussed in Section VI; in addition, it directly illustrates the effect of period on power loss and can help guide the choice of switching frequency. Starting at a low switching frequency, increasing frequency (and thus reducing the pulse width) decreases losses, but beyond a certain frequency, further increases not only result in diminishing returns, but actually increase core losses. This point corresponds to pulse widths

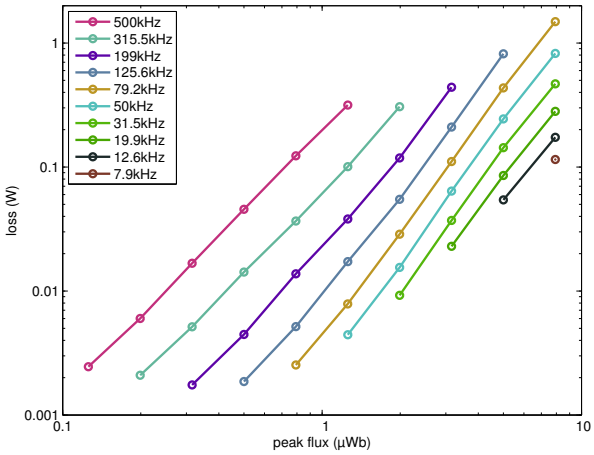

(a) Loss vs. peak flux parameterized by frequency

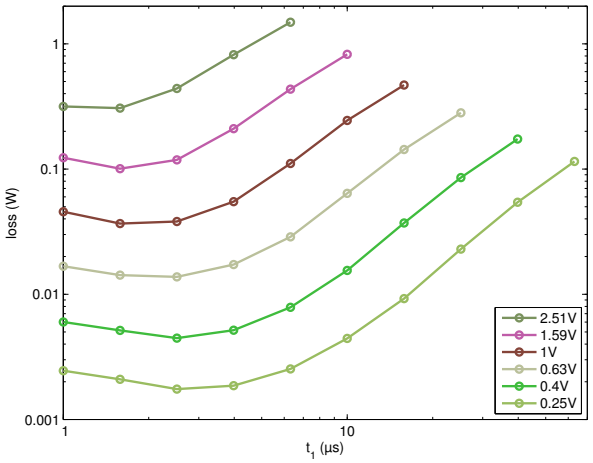

(b) Herbert curves: loss vs. on-time parameterized by voltage per turn

Fig. 3: Square-wave loss data for the ferrite core in Table I presented in two different formats.

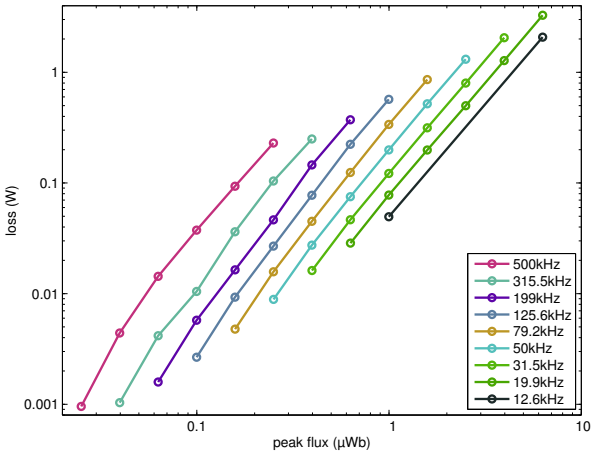

(a) Loss vs. peak flux parameterized by frequency

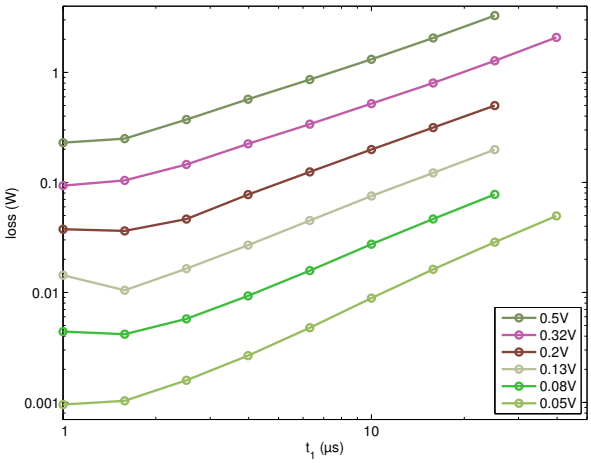

(b) Herbert curves: loss vs. on-time parameterized by voltage per turn

Fig. 4: Square-wave loss data for the powdered-iron core in Table I presented in two different formats.

of 1.5 to 3 μs for the ferrite material tested, and thus periods of 3 to 6 μs, and square-wave frequencies of 167 to 333 kHz. This is generally consistent with the behavior seen in plots of "performance factor" $B \cdot f$ for fixed power loss provided by some manufacturers [28], [29], [30]. However, the frequency beyond which performance degrades is lower in our data than in plots of performance factor for the same material (about 600 kHz [28]), presumably because of the harmonic energy content of the square-wave excitation.

Square-wave loss data for the powdered-iron core is shown in the same two formats in Fig. 4, and shows similar trends though the values are different.

B. Verification

Additional data was collected to assess the accuracy of the method described in Section III for predicting loss for other waveforms using only data from square-wave measurements. The first category of these tests is experiments using asymmetric waveforms as shown in Fig. 1(b) (upper right). The results of these experiments are plotted in Fig. 5. Each curve is for fixed width and amplitude of the first pulse (fixed V_1 and t_1 as defined in Fig. 1(a)) with the width of the second pulse (t_2) varying. The amplitude of the second pulse was adjusted for zero average voltage. The widths and amplitudes were all chosen to match data in the original characterization data set such that no interpolation was needed to predict loss, and the energy loss per cycle could be predicted from two points in the characterization data: the energy loss per cycle for a square wave of amplitude V_1 and half-period t_1 ($E_{\text{sqr}}(V_1, t_1)$) and the energy loss per cycle for a square wave of amplitude V_2 and half-period t_2, as

$$E_c = \frac{1}{2}\left(E_{\text{sqr}}(V_1, t_1) + E_{\text{sqr}}(V_2, t_2)\right) \tag{2}$$

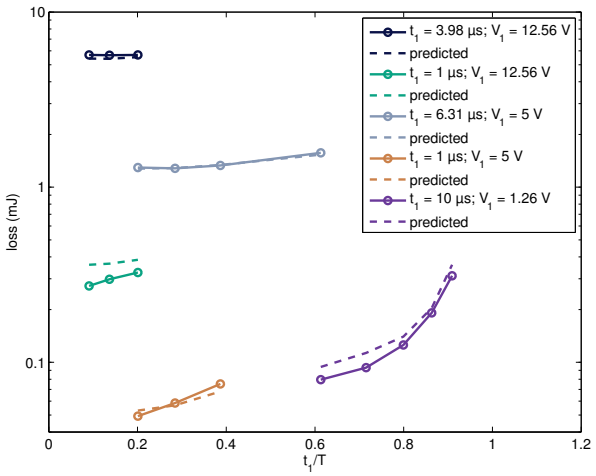

(a) Ferrite Core

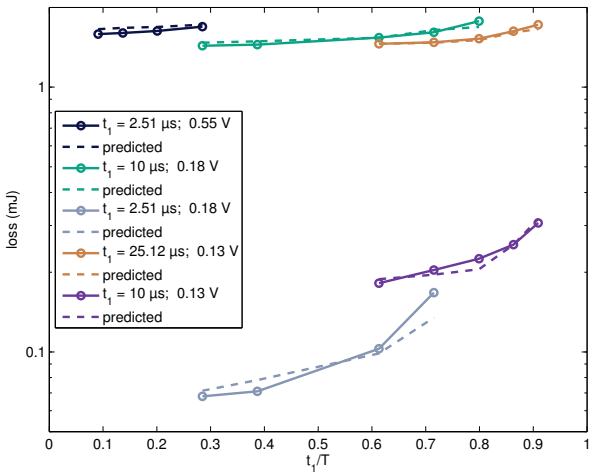

(b) Powdered-Iron Core

Fig. 5: Losses with asymmetric waveforms as predicted by the proposed approach compared to measured results.

The measured asymmetric waveform loss is compared to loss predicted from (2) in Fig. 5, showing excellent matching over a wide range of asymmetry ratios (t_1/T) and amplitudes, for both the ferrite core and the powdered iron core. This confirms that the composite waveform hypothesis is a good approximation for asymmetric waveforms.

Test results for waveforms with a zero-voltage time t_0 between pulses are shown in Figs. 6 and 7. In each test, the positive and negative voltage pulses have constant amplitude and duration (as listed in the figure legend), but the zero-voltage time between pulses, t_0, is varied. In Figs. 6(a) and 7(a), the waveform is always symmetric and the overall period is expanded as t_0 is increased (marked "Symmetric, $D < 1$" in Fig. 1(b)). In Figs. 6(b) and 7(b), the period remains constant but the waveform is skewed with one of the two zero-voltage periods shrinking as the other expands (marked "Shifted, $D < 1$" in Fig. 1(b)).

Based on the composite waveform hypothesis (see Section III), we would expect Figs. 6(a) and 7(a) to show constant energy loss per cycle as the zero-voltage time, and thus the period, increases, with no loss occurring during the zero-voltage time. The data in Fig. 6(a), for the ferrite core, show significant variations as t_0 increases, as much as about 40%, in some cases increasing and in others decreasing. The data in Fig. 7(a), for the powdered-iron core, show much less variation, matching the expectation from the composite waveform hypothesis very closely, with only slight increases in loss for long off-times, which may be a result of measurement artifacts.

The results for the shifted pulse waveforms, in Figs. 6(b) and 7(b), show little variation in loss as the pulse position is shifted (increasing one off-time while decreasing another), as would be expected from the composite waveform hypothesis, but the ferrite-core loss is slightly different from that predicted from the square-wave characterization data using (2), whereas the powdered-iron core matches the predicted loss more closely. This is consistent with the results shown in Figs. 6(a) and 7(a). For the ferrite core, the relatively low variation in loss as the pulse position shifts, compared to that shown in Figs. 6(a) and 7(a), could be explained by the effects of one off-time increasing offsetting the effect of the other decreasing for a net zero effect on loss. Alternatively, if the trends shown in Figs. 6(a) and 7(a) are due to measurement artifacts associated with the expanding period, this could also explain the relatively flat behavior seen in Figs. 6(b) and 7(b), because the shifted pulse experiments are immune to any errors associated with waveform period. However, the difference in behavior between the two cores seen in Fig. 6(a) and 7(a) indicates that the trends seen in the data are in fact due to the true behavior of the cores, not to any unexpected measurement artifacts.

VI. Design

The loss data derived from square-wave measurements can be provided to a magnetics designer in various forms, including tabulated data or curve-fit functions for use in software, and various types of graphical presentation. The loss data can be presented as loss per unit volume, or as total loss for a specific core, to simplify calculations for the designer. Here we discuss working from graphical data in the "Herbert curve" format of Fig. 3(b). These curves are parameterized by voltage per turn applied to a winding. It's also possible to provide curves like this for a specific *component* with a given number of turns, parameterized by voltage.

In general, for waveforms as shown in Fig. 1(a), based on (2), one can calculate loss from a Herbert plot as

$$P = \frac{1}{T}\left(P_{\text{sqr}}(V_1/N, t_1)\cdot t_1 + P_{\text{sqr}}(V_2/N, t_2)\cdot t_2\right) \qquad (3)$$

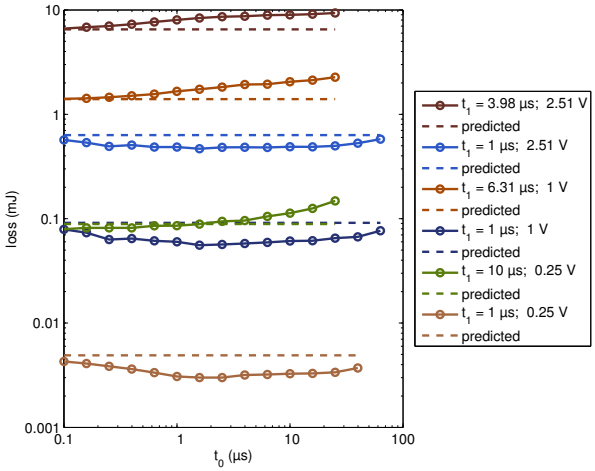

(a) Varying period

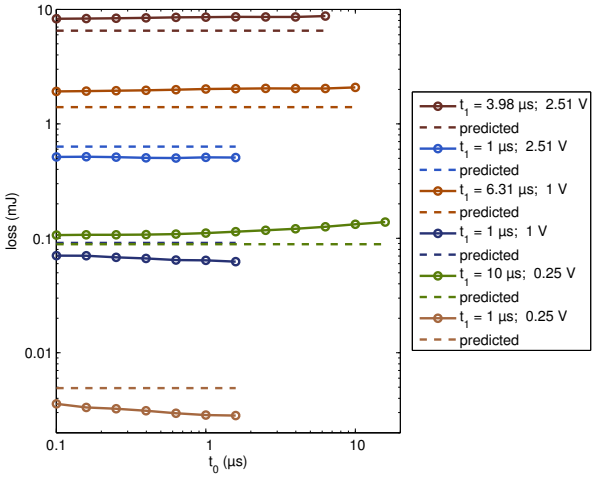

(b) Imbalanced off-times

Fig. 6: Experimental data testing the extension of ferrite-core square-wave data to waveforms incorporating zero-voltage time t_0. This is done by varying the period and extending off-time t_0, or by shrinking one zero-voltage time while expanding the other to maintain a constant period. The legend gives the on-time t_1 and the per-turn pulse voltage for each curve.

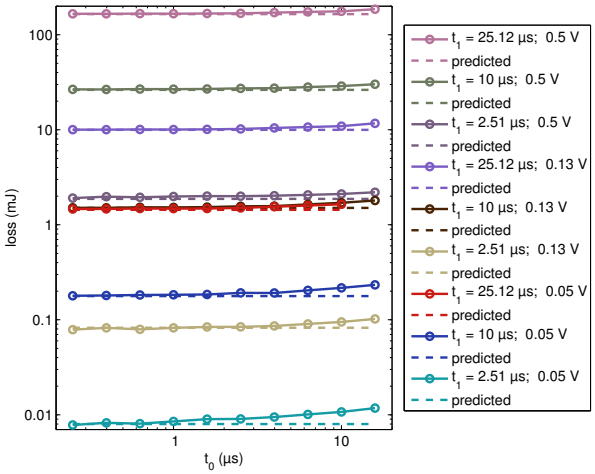

(a) Varying period

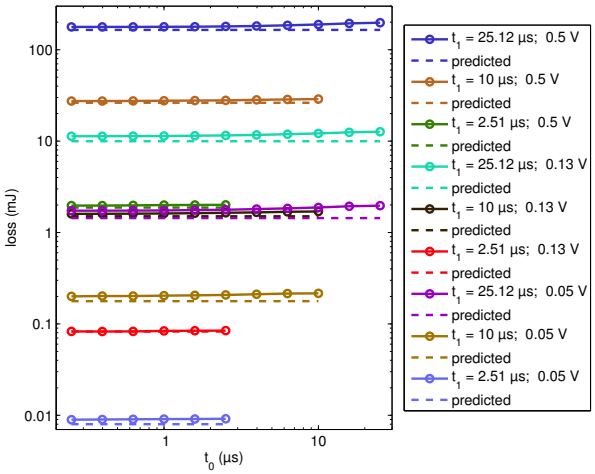

(b) Imbalanced off-times

Fig. 7: Experimental data testing the extension of powdered-iron-core square-wave data to waveforms incorporating zero-voltage time t_0. This is done by varying the period and extending on-time t_1, or by shrinking one zero-voltage time while expanding the other to maintain a constant period.

In the case of symmetric waveforms, $P_{\text{sqr}}(V_1/N, t_1) = P_{\text{sqr}}(V_2/N, t_2)$, and the loss calculation reduces to

$$P = \frac{2t_1}{T} P_{\text{sqr}}(V_1/N, t_1). \tag{4}$$

Consider, for example, a component operating at 50 kHz with a symmetric waveform with a duty cycle of 63%, 12 turns, and a pulse amplitude of 4.8 V. The period is 20 μs, and the positive and negative pulse widths are $t_1 = t_2 = 0.63 \cdot 10\ \mu\text{s} = 6.3\ \mu\text{s}$. To find the correct curve to examine in Fig. 3(b), we find the voltage per turn which is 4.8/12 = 0.4 V. As shown in Fig. 8, we can read off the power loss for this pulse width and voltage per turn as P_{sqr} = 7.9 mW. According to (4) we scale this result by the ratio $2t_1/T$ = 12.6 μs/20 μs, to get a predicted power loss of $7.9 \cdot 0.63 = 5$ mW.

An interesting design space to explore is to maintain constant frequency and average voltage, but to vary the pulse width and period. The relevant data is along a curve of constant volt-seconds on the Herbert plot—the dashed line in Fig. 9. To get power loss from these points, assuming constant frequency of 50 kHz, we then scale these points down by the ratio $2 \cdot t_1/20\ \mu$s to get the solid line in Fig. 9. This rise of this curve to the left illustrated the disadvantage of using shorter duty cycles for a given average voltage or volt-second requirement.

As an asymmetric example, consider the same 12-turn winding, with a 12 V, 10 μs pulse applied in one direction,

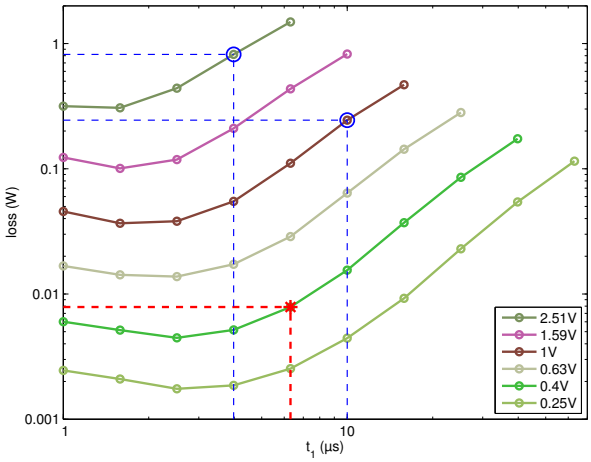

Fig. 8: Reading data from a Herbert plot for the examples discussed in the text. The lower red point marked with * is for the first, symmetric example. The upper blue circles are for the second, asymmetric example.

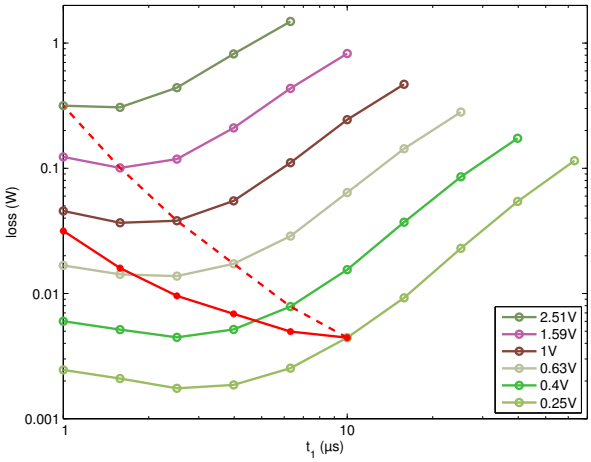

Fig. 9: Example exploring different duty cycle options for a constant average voltage (constant volt-seconds). The dashed line is the raw data points used from the plot; the solid line shows the result scaled by the ratio of on-time to period to calculate actual loss, as discussed in the text.

and a 30 V, 4 μs pulse applied in the other direction, with a 20 μs overall period (50 kHz) as before (the waveform includes a total of 6 μs of zero-voltage time). $P_{\mathrm{sqr}}(V_1/N, t_1)$ and $P_{\mathrm{sqr}}(V_2/N, t_2)$ are read off Fig. 8 as 244 mW and 818 mW. The overall power loss can then be found from (3) as

$$P = 50\ \mathrm{kHz}\,(244\ \mathrm{mW}\cdot 10\ \mu\mathrm{s} + 818\ \mathrm{mW}\cdot 4\ \mu\mathrm{s}) = 286\ \mathrm{mW}. \quad (5)$$

VII. Discussion

The results in Figs. 5 and 5(b) show that the composite waveform hypothesis holds well for asymmetric waveforms, and the method provides excellent accuracy. Fig. 7 shows that, for the powdered-iron core tested, it also holds very well for waveforms with zero-voltage periods, although zero voltage times can cause significant deviation in the ferrite core tested. This variation is not predicted by the composite-waveform hypothesis; nor is it predicted by any of the methods discussed in Section II. Additional work to better characterize and model this behavior could lead to more accurate loss predictions. However, even with this error, the approach described here is expected to be more accurate than other methods which are subject to the same error, and additionally entail error due to using sinusoidal data to predict square-wave loss.

In addition to being more accurate than other methods, the new approach is also easier to use than methods like the iGSE. Thus, we believe that it would be beneficial for core manufacturers to characterize square-wave loss and provide that data graphically, electronically or both, either on a per-unit-volume basis or on a per-core basis.

As presented here, the method is only applicable to waveforms with one positive voltage pulse and one negative pulse. However, it could also be easily applied to waveforms with minor loops by separating the minor loops following the approach in [6], as long as each constituent loop comprises only one positive pulse and one negative pulse. Adapting the method to waveforms with a series of voltage pulses of the same polarity but differing amplitudes is less straightforward. The corresponding analysis in the iGSE (eq. (13) in [6]) includes a factor that depends on the total flux excursion as well as the flux change for a given pulse, and it may be necessary to introduce similar factors to accurately model losses in such cases using square-wave loss data. However, most power electronics applications use waveforms with only one positive voltage pulse and one negative pulse, such that that the analysis here applies directly.

VIII. Conclusion

The proposed measurement and loss calculation approach allows generalizing square-wave core-loss data to predict core loss with any common rectangular voltage waveform. An automated measurement system has been used to collect the required square-wave core characterization data for ferrite and powdered-iron cores, and to collect additional data to assess the accuracy of the method for other voltage waveforms. Measurements show good correlation, but also exhibit behavior not yet explained by published models, which may lead to new insights and more accurate models. Despite the minor discrepancies, the loss prediction method yields higher accuracy, and is easier to use, than other methods for non-sinusoidal waveforms.

IX. Acknowledgements

Thanks to the Power Sources Manufacturers' Association and the National Institute for Standards and Technology (NIST) for support of this work.

References

[1] M. Albach, T. Durbaum, and A. Brockmeyer, "Calculating core losses in transformers for arbitrary magnetizing currents a comparison of different approaches." in *27th Annual IEEE Power Electronics Specialists Conference*, vol. 2, Jun. 1996, pp. 1463–8.

[2] J. Reinert, A. Brockmeyer, and R. De Doncker, "Calculation of losses in ferro- and ferrimagnetic materials based on the modified Steinmetz equation," in *Proceedings of 34th Annual Meeting of the IEEE Industry Applications Society*, 1999, pp. 2087–92 vol.3.

[3] A. Brockmeyer, "Dimensionierungswekzeug für magnetische bauelemente in stromrichteranwendungen," Ph.D. dissertation, Aachen University of Technology, 1997.

[4] J. Liu, T.G. Wilson, Jr., R. Wong, R. Wunderlich, and F. Lee, "A method for inductor core loss estimation in power factor correction applications," in *Proceedings of APEC 2002 - Applied Power Electronics Conference and Exposition*, 2002, p. 439.

[5] Jieli Li, T. Abdallah, and C. R. Sullivan, "Improved calculation of core loss with nonsinusoidal waveforms," in *IEEE Industry Applications Society Annual Meeting*, 2001, pp. 2203–2210.

[6] K. Venkatachalam, C. R. Sullivan, T. Abdallah, and H. Tacca, "Accurate prediction of ferrite core loss with nonsinusoidal waveforms using only Steinmetz parameters," in *IEEE Workshop on Computers in Power Electronics*, 2002.

[7] A. Van den Bossche, D. Van de Sype, and V. Valchev, "Ferrite loss measurement and models in half bridge and full bridge waveforms," in *IEEE Power Electronics Specialists Conference*, June 2005, pp. 1535–1539.

[8] A. van den Bossche and V. Valchev, *Inductors and Transformers for Power Electronics*. Taylor and Francis Group, 2005.

[9] S. Mulder, "Power ferrite loss formulas for transformer design," *Power Conversion & Intelligent Motion*, vol. 21, no. 7, pp. 22–31, Jul. 1995.

[10] E. C. Snelling, *Soft Ferrites, Properties and Applications*, 2nd ed. Butterworths, 1988.

[11] C. P. Steinmetz, "On the law of hysteresis," *AIEE Transactions*, vol. 9, pp. 3–64, 1892, reprinted under the title "A Steinmetz contribution to the ac power revolution", introduction by J. E. Brittain, in *Proceedings of the IEEE* 72(2) 1984, pp. 196-221.

[12] A. Brockmeyer, "Experimental evaluation of the influence of dc-premagnetization on the properties of power electronic ferrites," in *APEC '96. Eleventh Annual Applied Power Electronics Conference*, 1996, pp. 454–60.

[13] A. Brockmeyer and J. Paulus-Neues, "Frequency dependence of the ferrite-loss increase caused by premagnetization," in *Twelfth Annual Applied Power Electronics Conference and Exposition*, 1997, pp. 375–80.

[14] W. K. Mo, D. Cheng, and Y. Lee, "Simple approximations of the dc flux influence on the core loss power electronic ferrites and their use in design of magnetic components," *IEEE Transactions on Industrial Electronics*, vol. 44, no. 6, pp. 788–99, 1997.

[15] G. Bertotti, "General properties of power losses in soft ferromagnetic materials," *IEEE Transactions on Magnetics*, vol. 24, no. 1, pp. 621–630, 1988.

[16] ——, *Hysteresis in magnetism: for physicists, materials scientists, and engineers*. Academic Press, 1998.

[17] K. H. Carpenter, "Simple models for dynamic hysteresis which add frequency-dependent losses to static models," *IEEE Transactions on Magnetics*, vol. 34, no. 3, pp. 619–22, 1998.

[18] J.-T. Hsu and K. Ngo, "A Hammerstein-based dynamic model for hysteresis phenomenon," *IEEE Transactions on Power Electronics*, vol. 12, no. 3, pp. 406–413, 1997.

[19] H. Saotome and Y. Sakaki, "Iron loss analysis of Mn-Zn ferrite cores," *IEEE Transactions on Magnetics*, vol. 33, no. 1, pp. 728–34, 1997.

[20] W. Roshen, "Ferrite core loss for power magnetic components design," *IEEE Transactions on Magnetics*, vol. 27, no. 6, pp. 4407–15, 1991.

[21] P. Tenant and J. J. Rousseau, "Dynamic model of magnetic materials applied on soft ferrites," *IEEE Transactions on Power Electronics*, vol. 13, no. 2, pp. 372–9, 1998.

[22] F. Fiorillo and A. Novikov, "An improved approach to power losses in magnetic laminations under nonsinusoidal induction waveform," *IEEE Transactions on Magnetics*, vol. 26, no. 5, pp. 2904–10, 1990.

[23] D. Jiles, "Frequency dependence of hysteresis curves in 'non-conducting' magnetic materials," *IEEE Transactions on Magnetics*, vol. 29, no. 6, pp. 3490–2, 1993.

[24] W. Shen, F. F. Wang, D. Boroyevich, and C. W. Tipton, "Loss characterization and calculation of nanocrystalline cores for high-frequency magnetics applications," *IEEE Transactions on Power Electronics*, vol. 23, no. 1, 2008.

[25] R. Ridley and A. Nace, "Modeling ferrite core losses," *Switching Power Magazine*, vol. 3, no. 1, pp. 6–13, 2002.

[26] C. Oliver, "A new core loss model," *Switching Power Magazine*, vol. 3, no. 2, 2002.

[27] E. Herbert, "User-friendly data for magnetic core loss calculations," Aug. 2008, http://fmtt.com/Coreloss2009.pdf.

[28] "Ferrite material selection guide," 2000, magnetics Division of Spang & Company, Bulletin No. FC-S1.

[29] "Soft ferrites and accessories, data handbook," 2009, Ferroxcube, Eindhoven, The Netherlands.

[30] "Ferrites and accessories: SIFERRIT materials," 2006, EPCOS AG, Munich, Germany.

[31] K. Carpenter and S. Warren, "A wide bandwidth, dynamic hysteresis model for magnetization in soft ferrites," *IEEE Transactions on Magnetics*, vol. 28, no. 5, pp. 2037–41, 1992.

[32] I. Mayergoyz, *Mathematical models of hysteresis*. Springer-Verlag, 1991.

[33] P. Han, G. R. Skutt, J. Zhang, and F. C. Lee, "Finite element method for ferrite core loss calculation," in *Applied Power Electronics Conference and Exposition*, vol. 1, 1995, pp. 348–353.